JOURNAL OF GEOPHYSICAL RESEARCH, VOL. 102, NO. D23, PAGES 28,575–28,588, DECEMBER 20, 1997

Trace gas measurements in coastal Hong Kong during the PEM-West B

T. Wang,[1] K. S. Lam, L. Y. Chan, and A. S. Y. Lee

Environmental Engineering Unit, Department of Civil and Structural Engineering, Hong Kong Polytechnic University, Hong Kong

M. A. Carroll [2]
Department of Atmospheric, Oceanic, and Space Sciences, University of Michigan, Ann Arbor

Abstract. O_3, CO, NO_y, and SO_2 were measured at a coastal site in Hong Kong (22°13'N, 114°15'E, 60 m MSL) during the Pacific Exploratory Mission-West B (PEM-West B) in February and March 1994. Average concentrations determined in this study were 34 ± 14 ppbv for O_3, 458 ± 130 ppbv for CO, 9.33 ± 7.84 ppbv for NO_y, and 1.31 ± 1.46 ppbv for SO_2. Their high and variable levels suggest that the study site was often under the impact of fresh continental emissions (including urban Hong Kong) during the season of continental outflow. Concentrations of these species were strongly influenced by the passage of cold fronts and troughs which periodically brought high levels of pollutants from the north. Outflow of continental air was indicated by dramatic changes in meteorological parameters and in the levels of trace gas species. CO appeared to be a good chemical indicator of changes of air mass type, and its variability may be attributed to the relative strength of the outflow and to the transport of urban plumes. Variations of NO_y and SO_2 appeared to be mainly dominated by local sources. O_3 was poorly and often negatively correlated with CO and NO_y, suggesting that air masses sampled in the study period were highly inhomogenous with respect to the chemical signatures and that O_3 was chemically titrated by anthropogenic pollutants during the early stages of continental outflow. Calculated isentropic trajectories captured large-scale changes of air masses, indicated also by surface meteorological and chemical data. Trajectory results offering finer resolutions would yield more insight into the histories of smaller-scale air masses. Finally, the reasons for apparent disagreement between trajectory results, surface winds, and sometimes chemical data require further investigation.

Introduction

The Asian Pacific Rim is currently the fastest economically growing region in the world. With such accelerated growth in the economy and in human population, emissions of NO_x, SO_2, hydrocarbons, and other anthropogenic pollutants have increased dramatically. For example, areas in the east Pacific Rim region including Japan, Korea, coastal areas of China, Taiwan, and Hong Kong, have emissions of SO_2 and NO_x similar to those of Europe and eastern North America [*Akimoto and Narita,* 1994]. Furthermore, it is anticipated that in the 21st century, this region will become the largest source of SO_2 and NO_x in the world [*Galloway,* 1989]. Such high and rapidly growing emissions of NO_x, SO_2, and other anthropogenic pollutants will have an adverse impact on regional air quality and may also have a significant impact on the chemistry of the atmosphere over the remote Pacific region. In recent years, a number of studies, including NASA's Pacific Exploratory Mission-West A (PEM-West A), have been conducted to study the abundance and distribution of important trace gases and aerosols in the western Pacific, the transport of O_3, combustion-based and industrial pollutants, and also the transport of dust storms from the Asian continent to the remote Pacific [e.g., *Prospero and Savoie,* 1989; *Savoie and Prospero,* 1989; *Merrill et al*, 1994; *Hatakeyama et al*, 1995; *Hoell et al.*, 1996]. There have been, however, relatively few studies conducted over the South China Sea region. On the other hand, rapid economic and industrial development in the southern parts of China and other Southeast Asian nations have caused concern as to whether and how these increased human activities will affect the environment of this region and all of East Asia as well. Therefore there is a need for systematic investigation of the distribution of trace gases and aerosols, especially for long-term monitoring of the trends in regional atmospheric composition change and assessment of the impact of growing anthropogenic activities on the remote Pacific atmosphere. In response to this need, a background air monitoring station was established by the Hong Kong Polytechnic University in a relatively remote setting in Hong Kong. During the study period of the PEM-West Phase B (February-March 1994), an intensive measurement campaign was conducted at this station, during which O_3, CO, SO_2, NO, NO_y (NO_y = NO + NO_2 + NO_3 + $2N_2O_5$ + HONO + HO_2NO_2, + PAN + HNO_3 + aerosol nitrate + other organic nitrates), and total and respirable suspended particulates were measured. In

[1]Formerly at Department of Atmospheric, Oceanic, and Space Sciences, University of Michigan, Ann Arbor.

[2]Also at Department of Chemistry, University of Michigan, Ann Arbor

Paper number 96JD03750.
0148-0227/97/96JD-03750$09.00

addition, measurements of aerosol number density, black carbon, scattering coefficient, and collection of aerosol samples were made by the University of Miami [J. M. Prospero et al., unpublished manuscript, 1997]. This paper focuses on the levels and variability of O_3, CO, SO_2, and NO_y observed in Hong Kong during the PEM-West B, their relation to meteorological parameters, and correlations among themselves. Seasonal variations of CO and O_3 at this site are separately discussed by *Lam et al.* [1996].

Experiment

General Characteristics of the Region

Figure 1 gives the location of the regional cities whose anthropogenic emissions may have an influence on the trace gas levels at the Hong Kong Polytechnic University air monitoring station located in Hong Kong.

Hong Kong is located near the South China coast (latitude: 22°N, Longitude: 114°E) and is bounded to the north by the huge land mass of the Chinese mainland, to the south and east by the South China Sea, and to the west by the Pearl Estuary. The territory has a complex terrain and its hilly regions make up about 70% of the total land area. The population of Hong Kong currently stands at 6.3 million, with a density of 5780 persons/km^2, making it one of the densest cities in the world.

Directly north of Hong Kong is Guangdong Province, which houses three of the most rapidly developing Special Economic Zones (SEZ) in China: Shenzhen, Zhuhai and Shantou. Situated 30 km north of Hong Kong is Shenzhen, home to approximately 4 million people, 300 km northeast of Hong Kong is Shantou, while Zhuhai is located on the opposite side of the Pearl Estuary, 70 km west of Hong Kong. Guangzhou, the capital of the province, is situated 120 km northwest.

Located 400 km away from Hong Kong is another SEZ, Xiamen which is situated in the province of Fujian. Taiwan is approximately 500 km east of Hong Kong. The Portuguese colony of Macau is located about 70 km west of Hong Kong on the opposite side of the Pearl Estuary.

Table 1 shows the annual emissions of SO_2, CO_2, and NO_x of the described region. These values are based on the 1987 emissions calculated by *Akimoto and Narita* [1994]. The data shown suggest that the NO_x and CO_2 emissions in Hong Kong are comparable to province-based values in South China, while the emission of SO_2 in Hong Kong is much less.

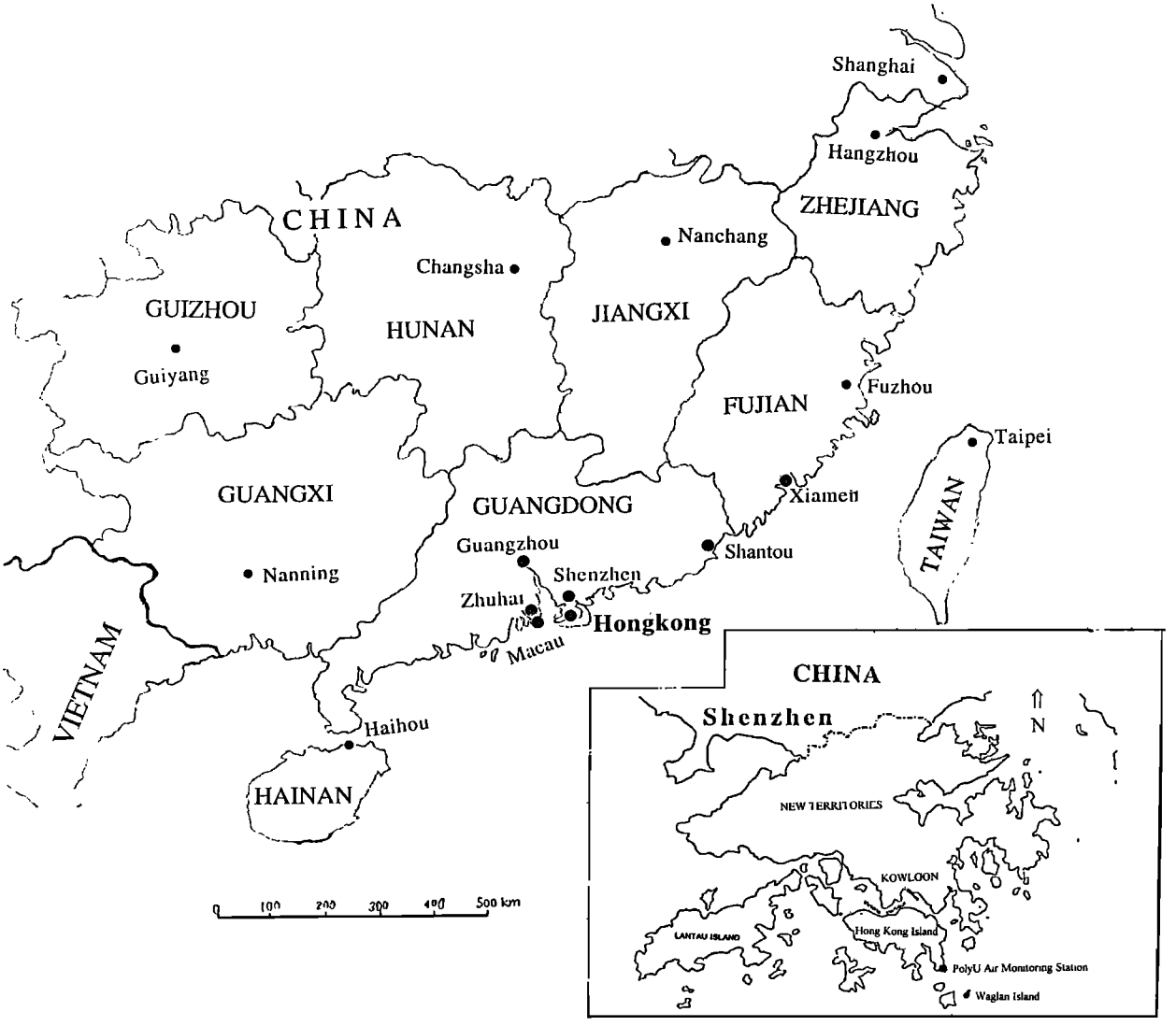

Figure 1. Map showing the study site in relation to Hong Kong and neighboring regions.

Study Site

The trace gas measurements were made at the Hong Kong Polytechnic University air monitoring station located at the southeastern tip of Hong Kong Island (Cape D'Aguilar, 22°13'N, 114°15'E, 60 m mean sea level (MSL); see Figure 1). This station is located in a relatively remote setting. The main population in the territory centers on Hong Kong Island (~1.3 million), Kowloon Peninsula (~2 million), and Shatin (~1 million) with an additional 2 million residents in the new towns and countryside. Urban centers are located northwest of the station. In the vicinity of the station, however, there are relatively few anthropogenic activities. The station is located near a Hongkong Telecom (HKT) facility, and there is only one restricted road (~4 km) to that facility. At the station, instruments were housed in a modified ship container located on a cliff 60 m above sea level. The HKT facility is located about 50 m south of the station and at a lower altitude. Facing south and east of the station is the South China Sea. During the winter season, prevailing winds are from the north and northeast, bringing in air pollutants from the Chinese mainland. Occasionally, urban plumes affected the levels of atmospheric species observed at the station. Local sources of pollution that may potentially affect the trace gas levels at the station include (1) emissions associated with activities in a small village and a small residential facility located about 1 km west of the station, (2) exhaust of the HKT emergency generator, which is tested once every two weeks, (3) exhaust from occasional vehicle traffic by personnel of the HKT and the station, (4) exhaust from small boats in the nearby ocean and from ocean liners which pass approximately 6 km south of the station, and (5) exhaust from commercial aircraft, whose routes are approximately 1 km east of the station and at altitudes of about 1 km. It appeared that exhaust from ships was the most important local source during the period of this study, since the other sources were normally not upwind of the station.

Instrumental Methods

Sampling inlets were mounted on a tower adjacent to the container and are approximately 4 m above the cliff.

Ozone. Ambient O_3 was measured with a UV photometric analyzer (Thermo Environmental Instruments Inc., Franklin, Massachusetts, model 49). It has a detection limit of 2 ppbv (signal to noise ratio = 2) and a precision of 2 ppbv.

Carbon monoxide. CO was detected with an infrared gas filter correlation analyzer (Thermo Environmental Instruments Inc., Franklin, Massachusetts, model 48S) with selected photomultiplier tube (PMT) for enhanced sensitivity. The analyzer was modified by adding a catalytic converter containing palladium heated to 250°C (0.5% Pd on alumina, type E221 P/D catalyst, Deggussa Corp., Plainfield, New Jersey) for instrument background determinations, as this modification was proven necessary for low-level CO measurements since the analyzer is sensitive to water vapor in ambient air [*Parrish et al*, 1991, 1994]. The detection limit (signal to noise ratio = 2) was estimated to be ~18 ppbv for 2-min integration time, and the precision (95% confidence) was approximately 20 ppbv for ambient levels of ~600 ppbv.

Sulfur dioxide. SO_2 was measured by using a pulsed UV fluorescence analyzer (Thermo Environmental Instruments Inc., Franklin, Massachusetts, model 43S) with selected PMT. A KOH-impregnated filter was added to determine the instrument background [*Parrish et al.*, 1991]. According to the manufacturer's specification, the detection limit for this analyzer is 0.06 ppbv for a 2-min integration, and the precision is 0.10 ppbv.

Total reactive nitrogen. A chemiluminescence analyzer (Thermo Environmental Instruments Inc., Franklin, Massachusetts, model 42S) was used to measure NO_y. The original molybdenum converter was relocated to the inlet system. In order to minimize the loss of "sticky" HNO_3 (a component of NO_y), the inlet (5 inch long, stainless steel) prior to the catalytic converter was heated to 100°C. The detection limit, as specified by the manufacturer, is 0.05 ppbv for 2-min average.

Instruments were calibrated regularly by adding a small flow of standard gas to the ambient airstream at the sampling inlet. For the O_3 analyzer an accurate O_3 source mixed in zero air was added at the sampling inlet to check if there was any loss of O_3 in the sample line. A flowing NO_2 standard obtained from titration of the NO standard was used to check the conversion efficiency of the molybdenum catalyst. For CO, SO_2, and NO_y, since their respective ambient levels were highly variable during the study period, calibration results were examined, and those affected by ambient variability were removed before the mixing ratios were calculated.

In addition to the routine calibrations, every 24 hours, scrubbed ambient air from a zero air generator (Thermo Environmental Instruments Inc., Franklin, Massachusetts, model 111) was used to check possible instrument bias and contamination of the sampling system. The results show that signals obtained from these artifact tests were low and negligible as compared with the ambient levels. During these tests, conversion efficiencies of palladium catalyst with respect to CO and of KOH filter with respect to SO_2 were determined Most of the time they exceeded 98%.

One-minute averaged data were collected with a data logger (Environmental Systems Corporation, Knoxville, Tennessee), and automatic calibrations and tests were controlled using a computer. Data presented in this paper are hourly averaged values

Results and Discussion

The data presented here cover the period from February 17 to March 13, 1994. During this period, the meteorology of the east Pacific region was dominated by an intense low-altitude anticyclone over northern China and Siberia and a low pressure system over the Aleutian Islands, resulting in a northerly or northeasterly low-altitude flow over the East Asian coastal regions. Figure 2 shows a typical synoptic weather map from the Hong Kong Observatory (HKO) and the frequency distri-

Table 1. Annual Emissions* of SO_2, NO_x, and CO_2

Region	SO_2, Gg S yr^{-1}	NO_x, Gg N yr^{-1}	CO_2, Tg C yr^{-1}
Southern China			
Guangxi	229	37	9
Guangdong	264	80	21 3
Jiangxi	227	48	13.4
Hunan	275	82	25.7
Fujian	123	34	8.9
Hong Kong	75	40.7	9.4
Macau	4.2	1.5	0 3
Taiwan	302	98 8	26 3

* 1987 values from *Akimoto and Narita* [1994]

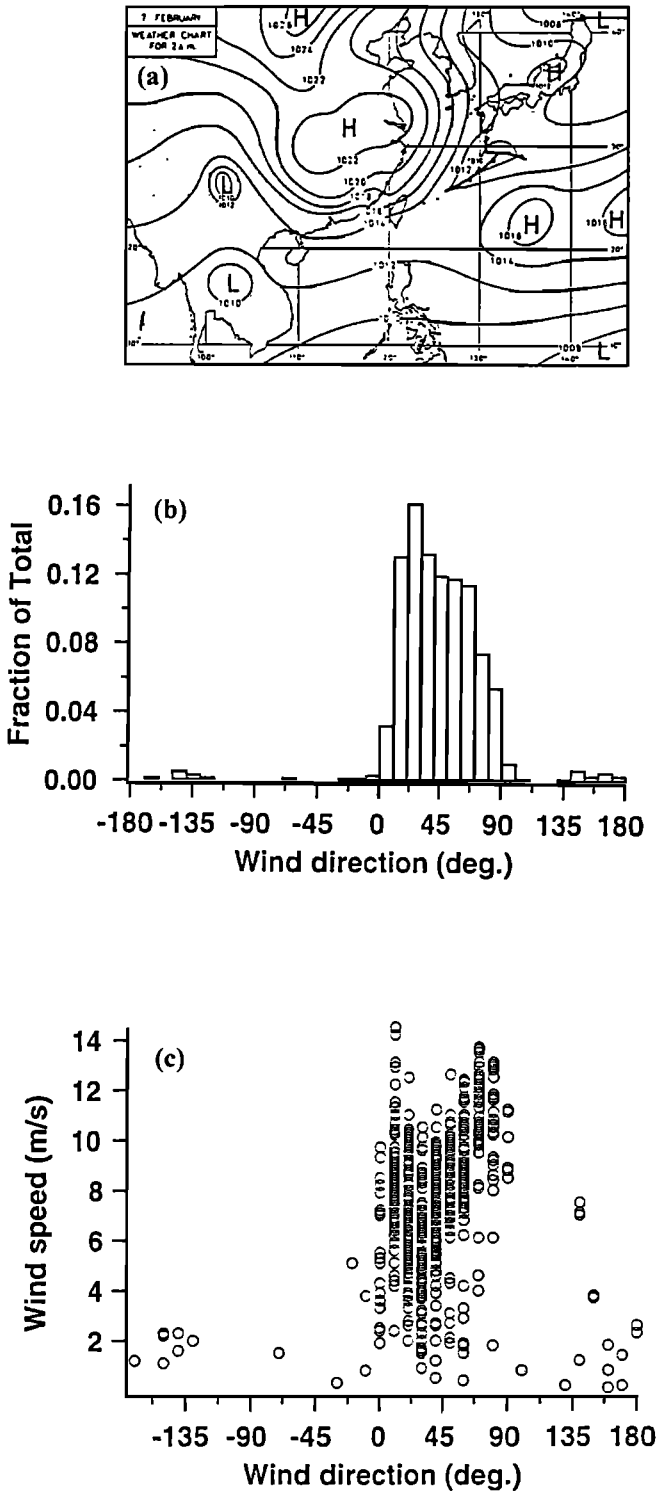

Figure 2. (a) Typical synoptic weather pattern during winter and spring in East Asia (chart reproduced with permission from the HKO's Monthly Weather Summary February 1994), (b) frequency distributions of surface winds recorded at Waglan Island, and (c) wind speed versus wind direction.

bution of the surface wind recorded at Waglan Island, which is approximately 5 km southeast of the station. The winds observed were predominantly from the north-northeast, with a few occasions when winds were from other directions.

Day-to-day Variations

Day-to-day variations of O_3, CO, NO_y, and SO_2 are shown in Figure 3, in conjunction with the time series of temperature, dew point, wind speed, and wind direction. In general, levels of O_3, CO, NO_y, and to a lesser extent, SO_2 were highly variable. SO_2 and NO_y variability was on a relatively short time scale, whereas CO showed both short- and long-time variations. Continental air periodically surged through Hong Kong, and changes of air mass types can be clearly seen in the following three consecutive periods.

Period 1: February 19-23. A wave of continental outflow started out late on February 19, with a cold front passing through Hong Kong. The air mass transition can be characterized by an obvious drop in air temperature and dew point and by dramatic changes in surface winds. Wind speeds decreased at first and resumed greater magnitudes following the passage of the cold front; wind directions turned more northerly during the frontal passage. This cold front brought to the study site highly concentrated pollutants from the north (urban Hong Kong and possibly other urban areas in China). For example, hourly average mixing ratios of CO increased sharply from ~450 ppbv to as high as 987 ppbv; NO_y increased from ~6 ppbv to 35 ppbv. The O_3 mixing ratio, on the other hand, dropped from about 30 ppbv to virtually zero, due to its chemical titration by NO_x. However, neither SO_2 nor black carbon [J. M. Prospero et al., unpublished manuscript, 1997] showed any significant enhancement during the passage of the front. This may be attributed to the washout of these pollutants by heavy rainfall on February 19. Following the passage of the cold front, prevailing northerly and northeasterly airflows resumed. Both temperature and dew point started to increase and the difference between them started to decrease until noon on February 24, when the air became relatively warm and humid, indicating that the outflow had reached a minimum. At the same time, CO levels gradually decreased, and ozone remained in the range of 40-50 ppbv; NO_y and SO_2 mixing ratios did not show such an obvious decrease as in the case of CO. The arrival of the dry continental air mass on February 19 brought the only sunny days observed in late February, namely, February 20 and 21.

Period 2: February 24 to March 8. The second cold front passed the South China coast on the evening of February 24. As in period 1, upon the arrival of the continental air mass, both temperature and dew point dropped and remained low until the period of March 6-8, when temperature and dew point started to increase. However, winds did not turn northerly during the frontal passage, so this cold front did not bring freshly emitted urban pollutants as was the case in period 1. Nevertheless, CO showed an obvious increase, while O_3 levels dropped sharply and remained low after the arrival of the continental air mass. On several occasions after February 27, winds turned northerly, and levels of CO and NO_y increased dramatically when ozone levels dropped. A pollution episode was observed on March 3 during which CO, NO_y, and SO_2 all exhibited significant increases. During this 1-day period, winds were from the southwest and the north, while wind speeds were low. Elevated levels of the pollutants on this day may be attributed to the transport of urban plumes in the relatively calm weather which enabled the pollutants to accumulate. Toward the end of period 2 (March 8), CO gradually reached the lowest levels observed during this study (~230 ppbv). Temperature and dew point reached their maxima; the

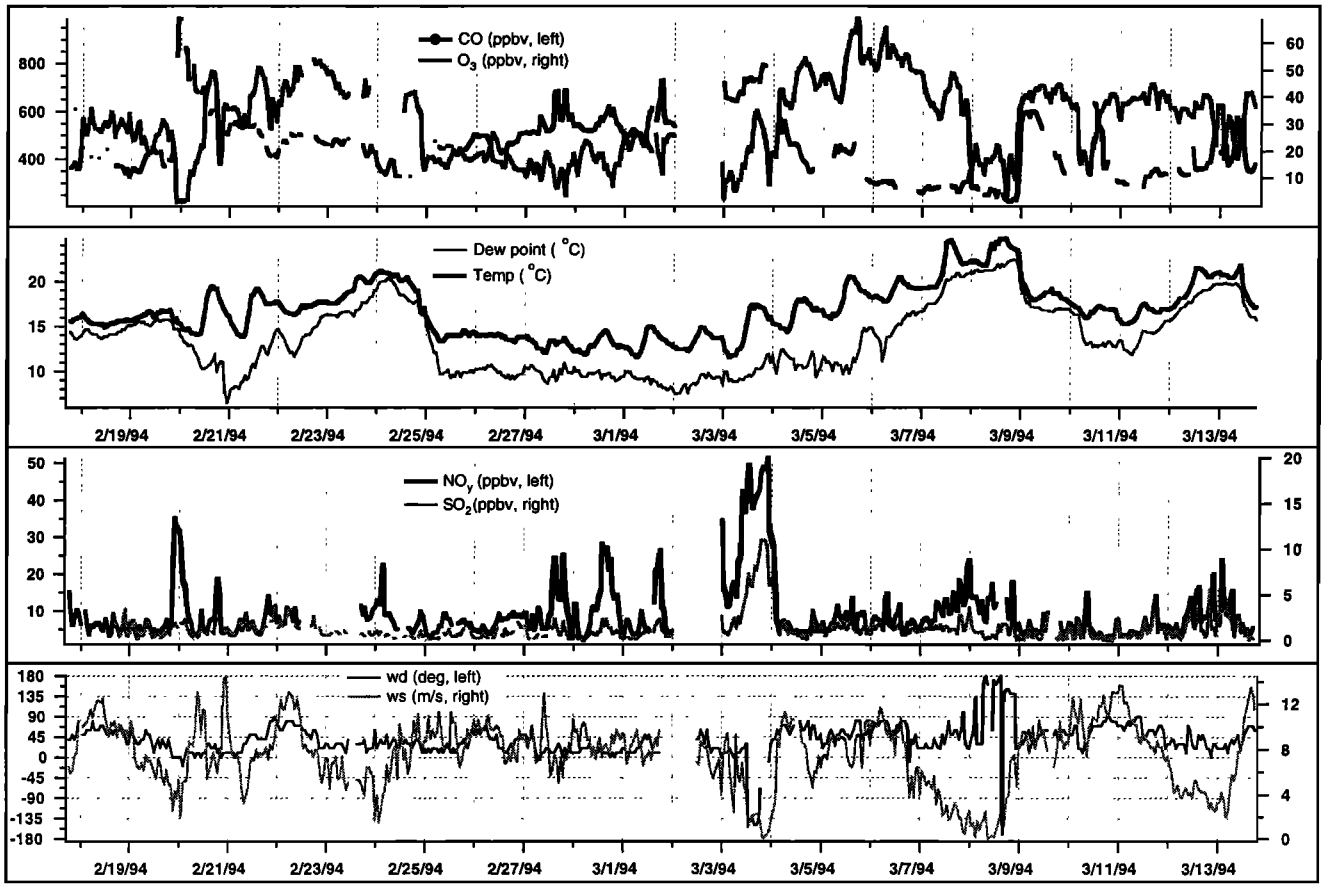

Figure 3. Time series of trace gas concentrations and meteorological parameters.

difference between them was reduced to a minimum. On March 8 winds switched to southerly and southeasterly and wind speeds were below 2 m/s. O_3 levels showed a sudden drop and remained low (~15 ppbv) on this day, and mixing ratios of NO_y were relatively high and variable. It appears that the low levels of O_3 on March 8 can be attributed to its titration by NO_x and other pollutants from sources upwind of the site as opposed to the arrival of a clean marine air mass, which would contain low levels of O_3. The following two pieces of evidence support this contention. First, low but variable O_3 levels coincided with enhanced and variable NO_y levels. Second, CO levels (300 ppbv) observed on this day were too high to be explained by the levels normally found in the background maritime conditions (~100 ppbv). The primary route for ocean liners in and out of Hong Kong lies to the south of the station, and emissions of NO_x from ships could have had a significant impact on the observed levels of NO_y at the site under low wind speeds.

Period 3: March 9-13. Both temperature and dew point showed sharp drops around midnight on March 9, when winds resumed a northeasterly direction (from southerly and southeasterly). It is noteworthy that such change in temperature and dew point was not associated with the passage of a cold front and that the concurrent enhancement in CO and O_3 levels was observed, whereas in the previous periods O_3 levels dropped significantly as the levels of CO increased. On March 10 a trough passed through the region, indicated by dropping temperature and dew point. During the passage of the trough, wind turned northerly, and CO and O_3 levels increased and decreased, respectively. In contrast to previous periods, the air masses observed during period 3 were relatively humid. Peaks in the levels of CO, O_3 (negative peaks), NO_y, and SO_2 were clear indications of influence by relatively fresh emissions and/or transport of urban pollutants.

Backward Air Trajectories

Calculated backward air trajectories are valuable in estimating the origin of an air parcel and the time spent by that parcel on a particular route since leaving a major anthropogenic source region. *Akimoto et al.* [1996] utilized isentropic trajectories as a way of classifying air masses to analyze the O_3 data measured during PEM-West A at three ground sites in the western Pacific including Oki Island and Okinawa of Japan and Kenting of Taiwan. Similarly, *Kajii and Akimoto* [this issue] employed the same air classification scheme to analyze their observations of O_3, CO, and acidic trace gases recorded at Oki during the PEM-West B. In this study we attempt to make use of the same isentropic back trajectories calculated by Merrill et al. [this issue] to confirm the outflow cycles inferred from the changes in temperature and dew point (as discussed in the previous section). However, several factors have to be considered with regard to the applicability of these trajectories to this study site, as well as the general limitation of the trajectory model [Merrill, 1996].

During winter and spring, the prevailing surface winds observed by the station are from the north and northeast. Quite often, air trajectories pass over polluted continental regions before reaching Hong Kong. Anthropogenic sources in this

region are unevenly distributed, as shown in Figure 1. Therefore we expect that air from the north may have a different chemical signature from the air coming from the northeast. Similarly, air from the northeast, along the coast, would be different in terms of the anthropogenic loading from air arriving from the east. In order to distinguish these trajectories, the trajectory model would need to provide fine spatial resolution. In addition, trajectory model results would need to be representative of surface flow so that they can be used as an aid for the interpretation of ground-based measurements (radiosonde data from the HKO (not shown) indicate that surface wind flow patterns can differ significantly from those observed at higher altitudes). Also, the complex terrain of Hong Kong makes it difficult to study the wind flow over the territory. With these concerns in mind and the fact that the available trajectories are intended for large-scale flow patterns, we examined these trajectories and compared them with the meteorological parameters and the time series of trace gases.

Three types of trajectories were observed: type I (Figure 4a) shows that the air comes directly from the north, perhaps crossing parts of urban Shenzhen and Hong Kong. An air mass of this type would contain high levels of pollutants. Type II (Figure 4b) indicates that the air mass leaves the east coast of China and travels for some period of time over the ocean before returning to the continent. An air mass of this type might be expected to have the characteristics of "aged" continental air and thus would contain lower levels of anthropogenic pollutants in comparison to those found in Type I. Type III (Figure 4c) suggests that the air mass originates from the western Pacific, moves westward over the Philippines, and proceeds to Hong Kong in a south-southwesterly direction. An air mass of this type could be the cleanest sampled over the study period.

A comparison of trajectory type with the respective surface data shows that the trajectories tended to capture the large-scale changes of air masses for periods after the arrival of continental air. For instance, for the period February 26 to March 4, the trajectories observed (see Figure 5a) suggest an air mass of a type I, and indeed, the recorded low temperature, low dew point, and high levels of CO, as well as the observed northerly-northeasterly winds, support this estimation. For March 5 and 7 the trajectories (see Figure 5b) suggest a type II air mass, spending approximately 1 - 1.5 days over the ocean. Again both chemical and meteorological data support this trajectory estimation: temperature and dew point increased and CO levels were reduced significantly (in a relative sense). It should be noted that there was much variability in trace gas concentrations (February 26 to March 4) which may be explained by the erratic changes in wind direction. Such variability is not clearly indicated by the trajectories.

On the other hand, there were periods (roughly 10 out of 24 days)when the calculated air trajectories and surface winds (and sometimes chemical signatures) did not agree with each other. They are the periods February 19, February 23-25, March 7-10, March 12-13, when the air trajectories suggest a type III air mass. Trajectories of this type suggest that the air reached Hong Kong from the south and southwest. However, the observed winds (except on March 7-8) at Waglan Island showed otherwise (i.e., northeasterly; see Figure 3). In addition, trajectories for February 25 and March 9-10 (Figure 5c) contradict the conclusions drawn from the chemical data as well as the surface wind, temperature, and dew point: the trajectories suggest the presence of a maritime air mass, but the chemical data strongly indicate an air mass of continental origin. We noticed that this disagreement (trajectories versus observed surface winds) occurred at the time of changing air masses (indicated by changes in temperature and dew point) and appeared to coincide with the arrival of cold fronts. Also, synoptic weather patterns observed during these periods were sometimes dominated by the presence of high and low multiple pressure systems in East Asia (see Figure 6 for an example). It is not clear whether the disagreement between the observed surface winds and trajectories is due to either the complicated synoptic weather patterns or the arrival of cold fronts, or simply due to the fact that the calculated trajectories are not representative of the observed surface wind flow patterns. This topic therefore requires further study.

In summary, the trajectories seem to have captured some features of the direct outflow of air from the north and the "aged" outflow of air from the east of the continent. However, the reason for the apparent disagreement between surface winds and the results of the trajectory model requires an in-depth study. For this study site a trajectory model with a finer spatial resolution would be useful in further characterizing air histories, as such resolution helps delineate each air mass arriving from the continent. Nevertheless, the calculated trajectories were able to capture the contrasting features of wintertime continental outflow and summertime inflow of maritime air [*Lam et al.*, 1996].

Comparison With Other Observations

The results of the trace gas concentrations at the station are summarized in Table 2. *Talbot et al.* [this issue] reported median mixing ratios for air parcels that had recently (< 2 days) left source regions (latitude > 20°N, altitude < 2 km) were 42, 186, 0.58, and 0.10 ppbv, for O_3, CO, NO_y, and SO_2, respectively. As discussed earlier, the lowest concentrations of trace gases (except for O_3) observed at the present site could be associated with relatively "aged" continental outflow (1-2 days, as determined by the calculated back trajectories). During such periods, O_3 levels were approximately 40 ppbv, and CO values were in the range of 221 to 300 ppbv. These values are comparable to Talbot's values. However, our SO_2 and NO_y values were much higher, presumably due to the influence of nearby sources. In addition, the NO_y levels at the present site were also higher than those measured at Oki Island during September-October 1991. In another study, *Kondo et al.* [this issue] reported that the NO_y mixing ratios recorded during boundary layer legs were in the range of 0.7 to 0.9 ppbv.

Arimoto et al. [this issue] compared CO and O_3 levels measured at Oki Island of Japan with those measured at the Hong Kong Polytechnic air monitoring station and on board a DC-8 plane during boundary layer flights. They found that, on average, CO levels in Hong Kong were higher than at Oki Island, while the opposite was found true for O_3. They noted that the pollutants detected in the air samples taken in Hong Kong and Oki Island may have been emitted from different parts of Asia and that the two stations receive different air asses from each other. Here it is worth noting that the Hong Kong station may have been under the impact of the emissions from South China i.e., in the upwind northeast directions of the station. Trace gas data are sparse over the South China Sea. During one boundary layer leg of flight 10 on February 21, the DC-8 flew over the South China Sea between 1517 and 1552 (local time). The CO recorded during this period of time was in the range of 250 to 422 ppbv and O_3 was 46-54 ppbv. For the

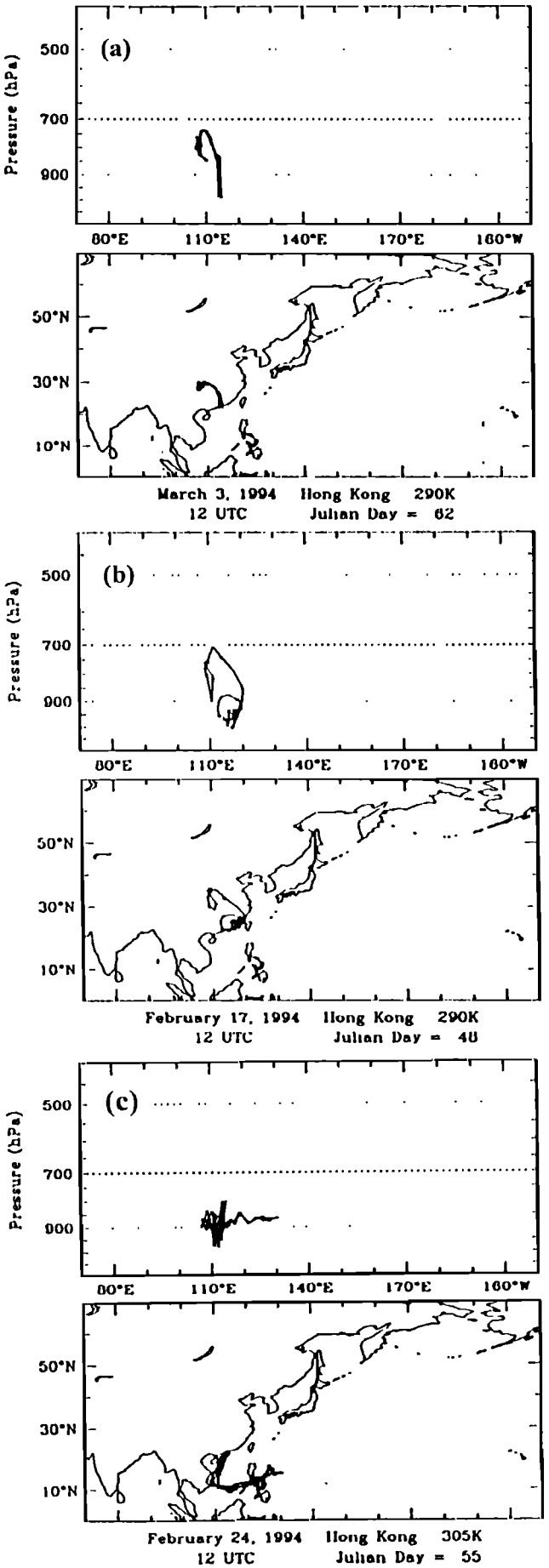

same period at the Hong Kong station, winds were from the north and northeast and the CO mixing ratio was ~500 ppbv and for O_3 about 50 ppbv. The O_3 levels recorded at the station and on the DC-8 were similar, but the CO levels were higher at the station. This difference may be due to the station's proximity to continental sources. In addition, *Arimoto et al.* [this issue] noted that, in contrast to the results found during another flight near Taiwan (flight 12), the CO and O_3 levels recorded for flight 10 were poorly correlated. They suggested that this was a reflection of the existence of several chemically distinct air masses. Interestingly, the data obtained in Hong Kong gave similar results (see below). In general, the correlation of CO and O_3 was poor, and there were no obvious indications of a positive correlation. These two sets of data indicate the large-scale inhomogeneity of the air masses sampled over the South China Sea region.

Interspecies Relationships

As noted in the previous sections, CO (as well as O_3) varied on both short and long timescales, whereas variations in NO_y and SO_2 levels were apparently dominated by short timescale processes. To further study the relationship among these chemical species, correlations of CO with NO_y, SO_2, and black carbon were examined and are presented in Figure 7, and correlation among NO_y, SO_2, and black carbon are shown in Figure 8. These scatter plots show that CO and NO_y are not correlated except for CO levels >600 ppbv, and CO is independent of SO_2 (except on one occasion on March 3) and black carbon. NO_y, SO_2, and black carbon, on the other hand, correlate reasonably well among themselves.

For CO >600 ppbv, the observed correlation between CO and NO_y on February 20 and the correlation of CO with both NO_y and SO_2 on March 3 are the reflection of the coexistence of emission sources of these pollutants in the urban areas.

For CO levels <600 ppbv (representing roughly the regional air mass characteristics during the study period), the lack of positive correlation of CO with NO_y, SO_2, and black carbon can be attributed to (1) different source origins and/or (2) differences in chemical lifetime and physical (wet and dry) removal rates of the pollutants from the atmosphere. CO has a chemical lifetime of more than 1 month and cannot be washed out or be subject to surface deposition. Therefore it can be transported over long distances. For NO_y, although its chemical lifetime can also be as long as 1 month [*Warneck*, 1988], some of its components (gaseous HNO_3 and nitrate) can be easily removed from the atmosphere by washout and through dry deposition. Similarly, SO_2 and black carbon are subject to these two physical removal processes, with the former being chemically transformed into sulfate in 0 2 days [*Warneck*, 1988]. For example, the washout of SO_2 by heavy rainfall on February 20 may have destroyed the correlation between CO and SO_2. As the study was conducted in the wet season of the year, and since there were apparent local sources of NO_y and SO_2, we attribute the variability in NO_y and SO_2 mainly to local sources rather than continental. On the other hand, the long-range transport of continental emissions may have significant influence on the CO levels observed at the station.

Another way to look at the representativeness of the data with respect to the regional characteristics is to apply a wind

Figure 4. Air mass classification: (a) type I for northerly flow, (b) type II for aged continental outflow, and (c) type III for marine air mass.

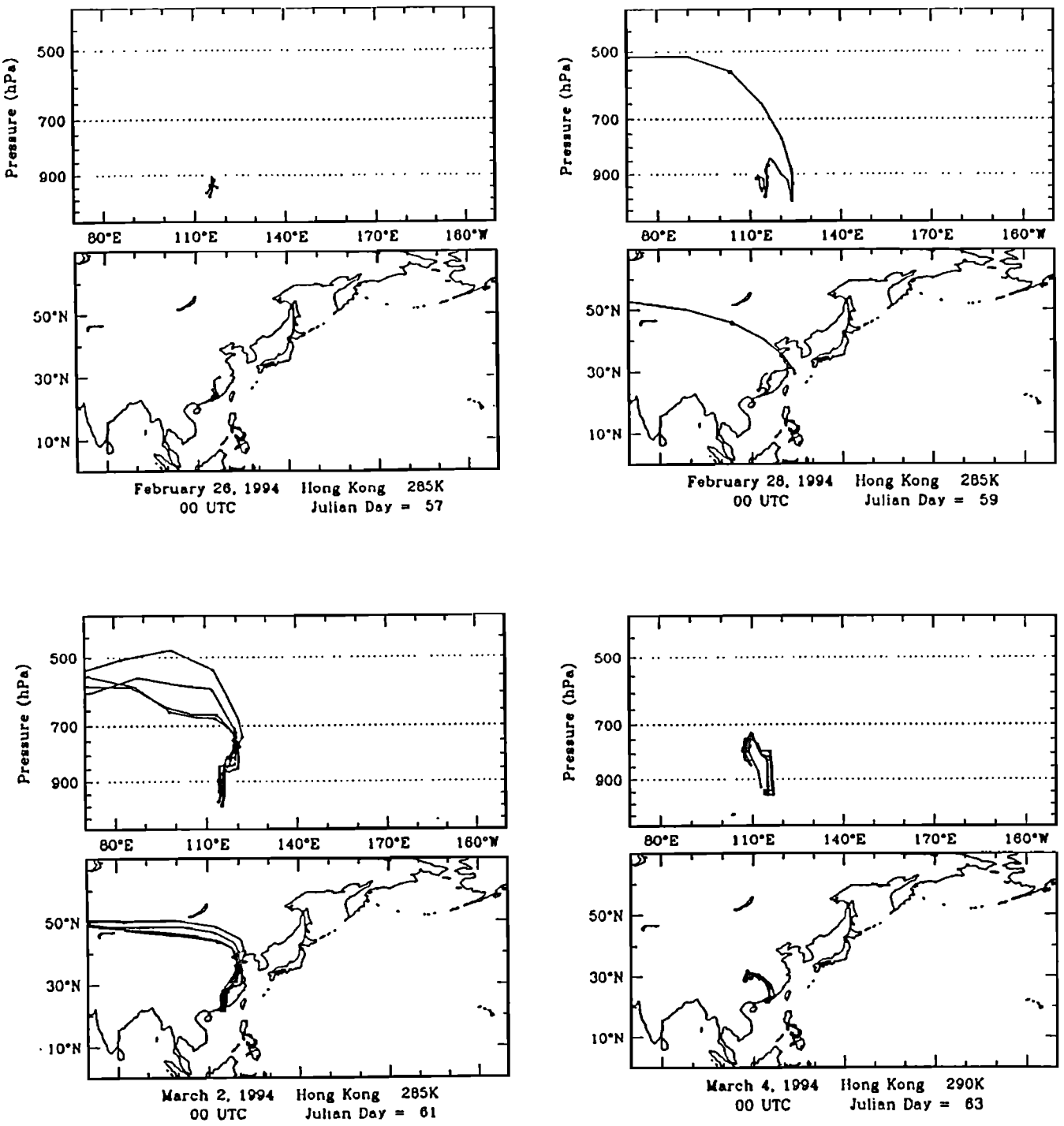

Figure 5. Back trajectories for (a) February 26 to March 4, (b) March 5-7, and (c) March 8-10.

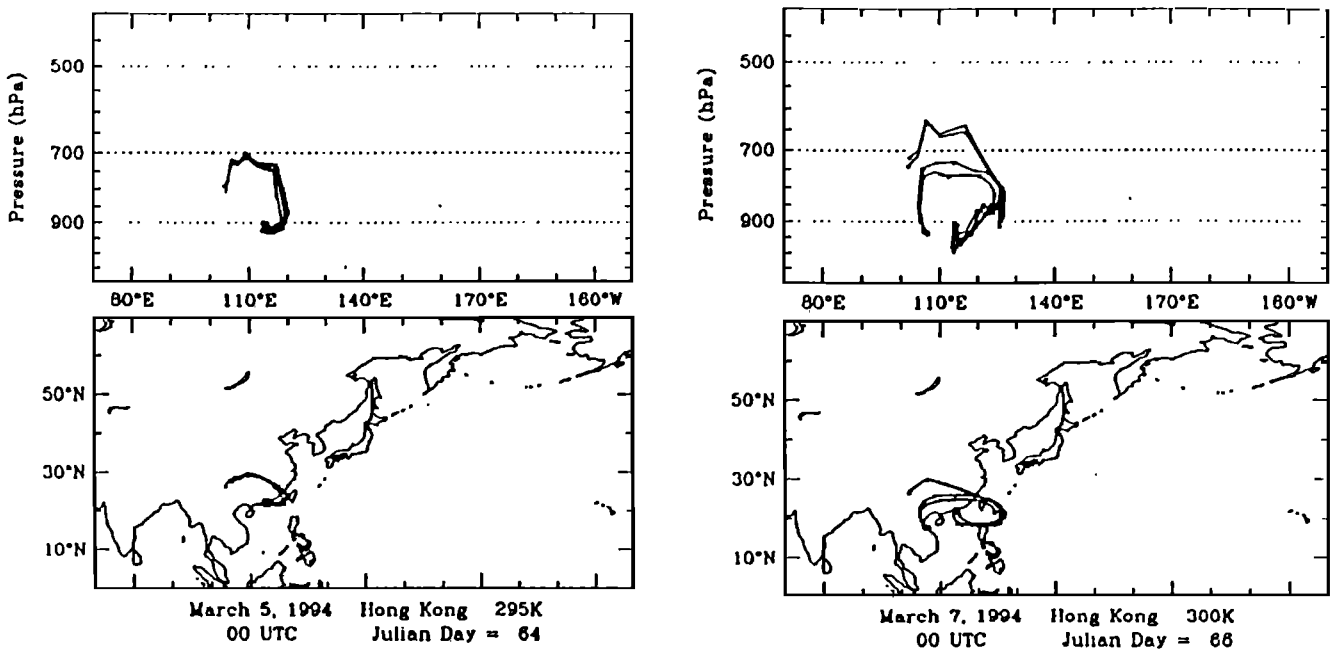

(b)

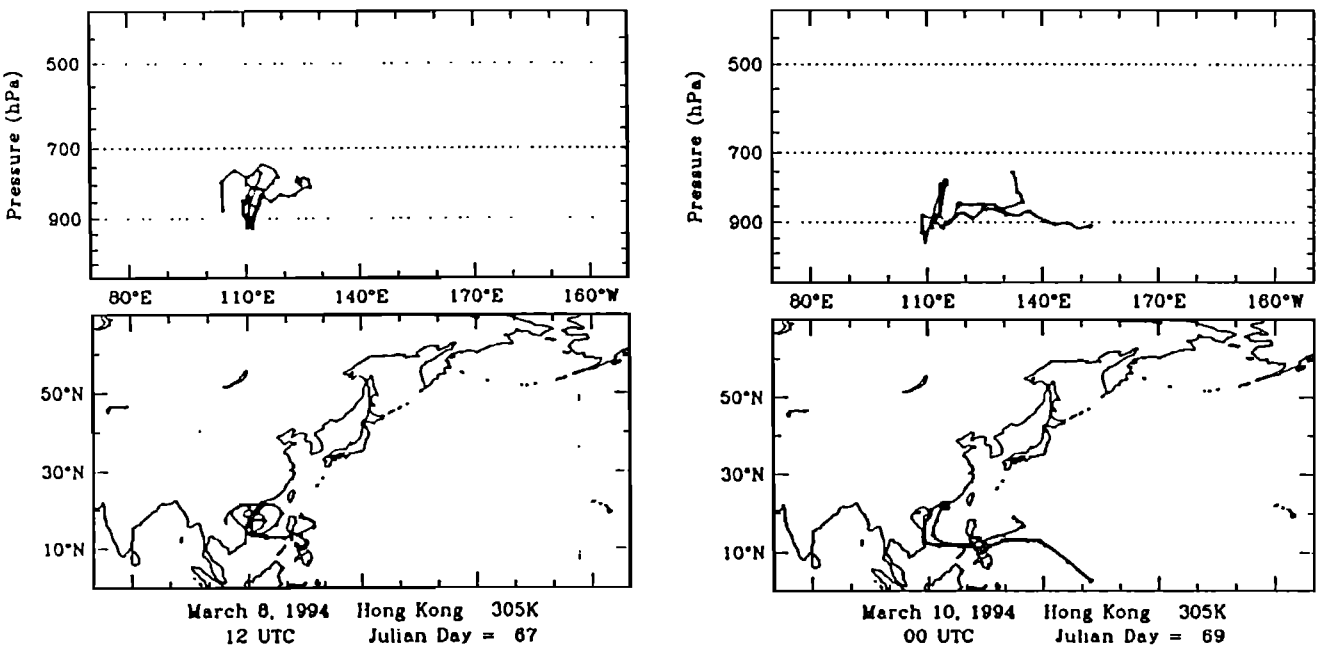

(c)

Figure 5. (continued)

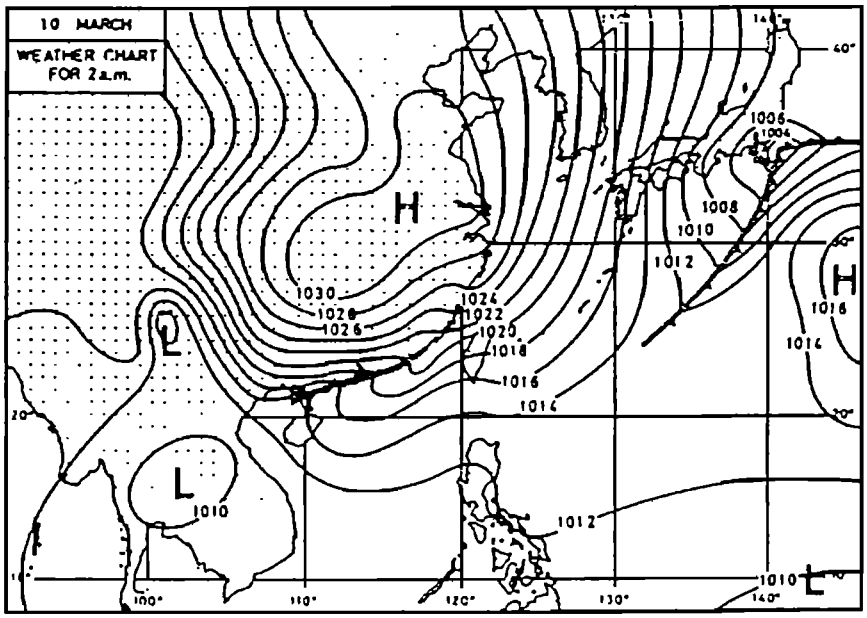

Figure 6. Synoptic weather map for March 10 (chart reproduced with permission from the HKO's Monthly Weather Summary March 1994).

filter to the data set. Here we focus on the periods with strong northeasterly and easterly winds (wind direction >40° and wind speed >5 m/s) and assume that data for these periods had less impact from urban emissions (mainly located north and northwest of the station). The correlation of CO with NO_y, SO_2, and black carbon is shown in Figure 9a. It is evident that CO has no correlation with NO_y, SO_2, and black carbon.

Reasonable correlation among NO_y, SO_2, and black carbon suggests a common source of origin. The correlation even exists for periods of strong northeasterly and easterly winds (Figure 9b). Considering their short resident time in the atmosphere, the existence of a correlation in the filtered data set must indicate the influence of local sources on the station. One of candidates for these local sources is the emission from ships. Intense activities in 1994 associated with the reclamation of the new airport (Chek Lap Kok) may have contributed to the unusually high frequency of ship sailings in the waters close to the station during the study period.

The relationship of O_3 between CO and NO_y was examined to elucidate wintertime and springtime O_3 chemistry. As seen in Figure 10a, O_3 is negatively correlated with both CO and NO_y, but such a correlation is not very strong. In the case of CO, it is noted that a group of data points with low values of O_3 and CO belongs to March 8 when surface winds were from the south-southeast and that, as discussed previously, the titration of O_3 by local sources upwind of the station reduced the secondary pollutant to low levels. The majority of the data is associated with periods of continental outflow. The overall negative O_3-CO correlation and observed high levels of CO indicates that, during the initial periods of continental outflow (lower right corner of figure 10a), O_3 is titrated by anthropogenically emitted NO_x and volatile organic compounds (here CO is a such tracer). The O_3-NO_y relationship is not as clear as observed for O_3 and CO, and the data are more scattered for NO_y levels below 10 ppbv. This would be expected if one assumes that some of the NO_y was lost during transport. Nevertheless, an overall negative O_3-NO_y correlation can be seen.

Table 2. Summary of Trace Gas Concentrations

Species	Mean (±s.d.*)	Median	Range	Number of points
O_3	34 (±14)	32	1- 67	526
CO	458 (±130)	455	221 - 987	409
NO_y	9.33 (±7 84)	7.01	1.98 - 51.5	508
SO_2	1.31(±1 46)	0 95	0.031 - 11.0	484

All concentrations are in units of ppbv.
* Standard deviation

Once again, in order to look at data of a more regional nature, we applied the wind speed and wind direction filters, and the subsequent correlation is shown in Figure 10b. The O_3-NO_y relationship becomes virtually uncorrelated, and O_3-CO is more scattered, but the overall negative correlation can still be seen. The lack of correlation between NO_y and O_3 can be understood if one considers the impact of NO_y from local sources (i.e., ship emissions). The lack of positive correlation between CO and O_3 in this subdata set suggests a variety of air masses were sampled, including those with different initial loading of pollutants and with varying degrees of photochemical processing.

In summary, the variability of CO and O_3 can be attributed to both short-range transport of local sources including urban/power plant plumes, and the transport of continental sources over long distances, whereas the elevated levels of SO_2 and NO_y were primarily determined by local sources. SO_2, NO_y, and black carbon correlated reasonably well, perhaps indicating a common origin.

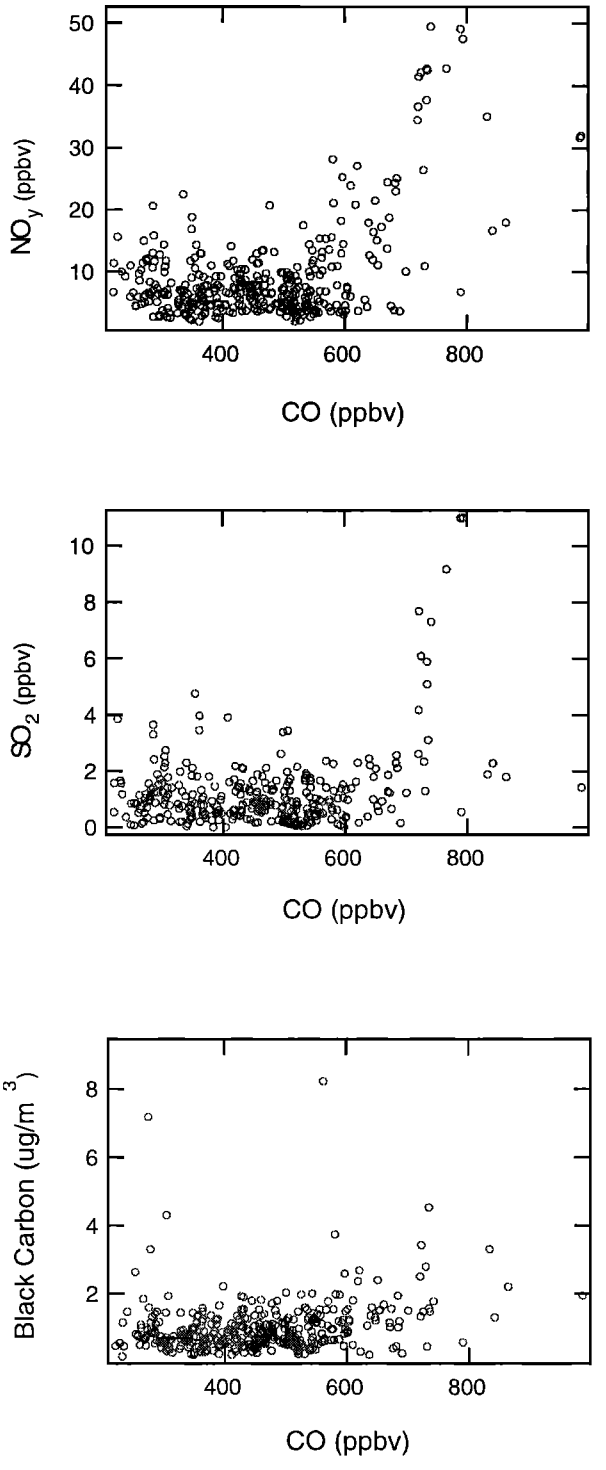

Figure 7. Relationships of CO with NO_y, SO_2, and black carbon.

Finally, in order to illustrate the influence of continental outflow on the background levels of trace gases at the station during the winter season and to demonstrate its capability of receiving regional background air mass, concentrations of CO and O_3 obtained during this study were compared with those obtained in June 1994. The results are summarized in Table 3. As indicated, the winter median mixing ratios of CO and O_3 are much higher than those observed in the summer despite the fact that pollution episodes occasionally affected the site during the summer season (indicated by relatively large means as compared with medians and large standard deviations). A more elaborate discussion on seasonal variations of these two species is given by *Lam et al.* [1996].

Conclusions

Trace gas species including O_3, CO, NO_y, and SO_2 were measured at a coastal air monitoring station in Hong Kong

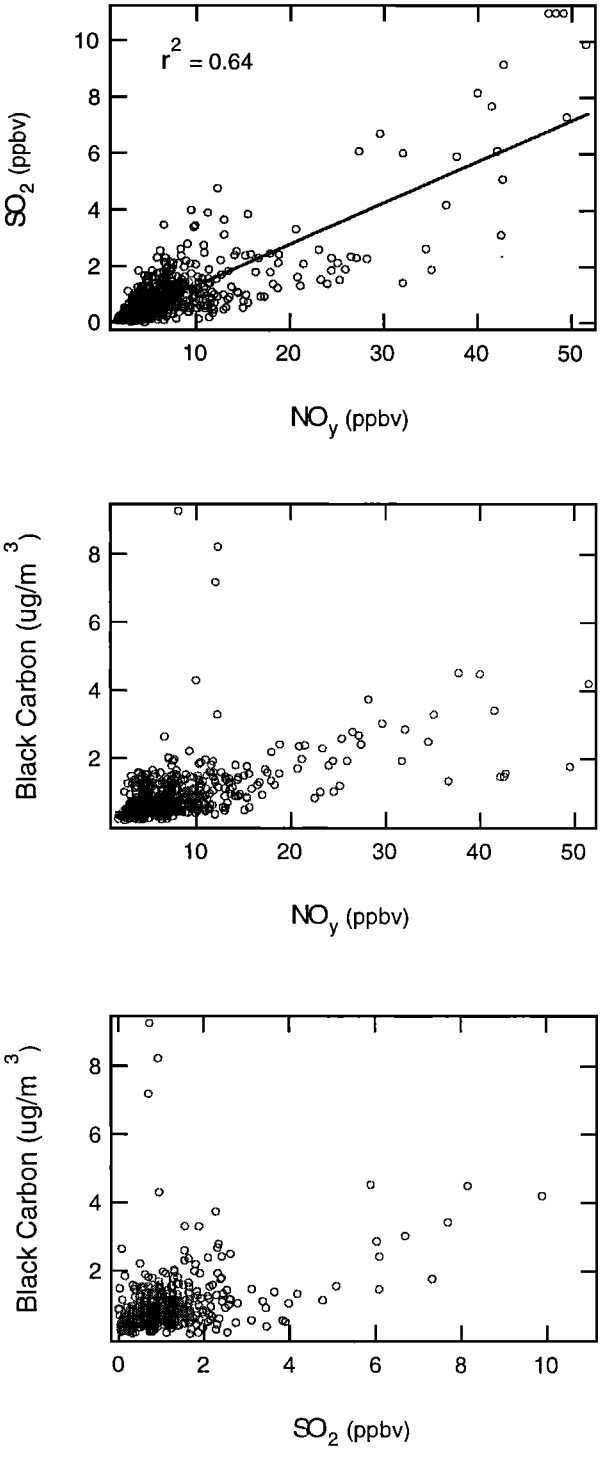

Figure 8. Relationships among NO_y, SO_2, and black carbon.

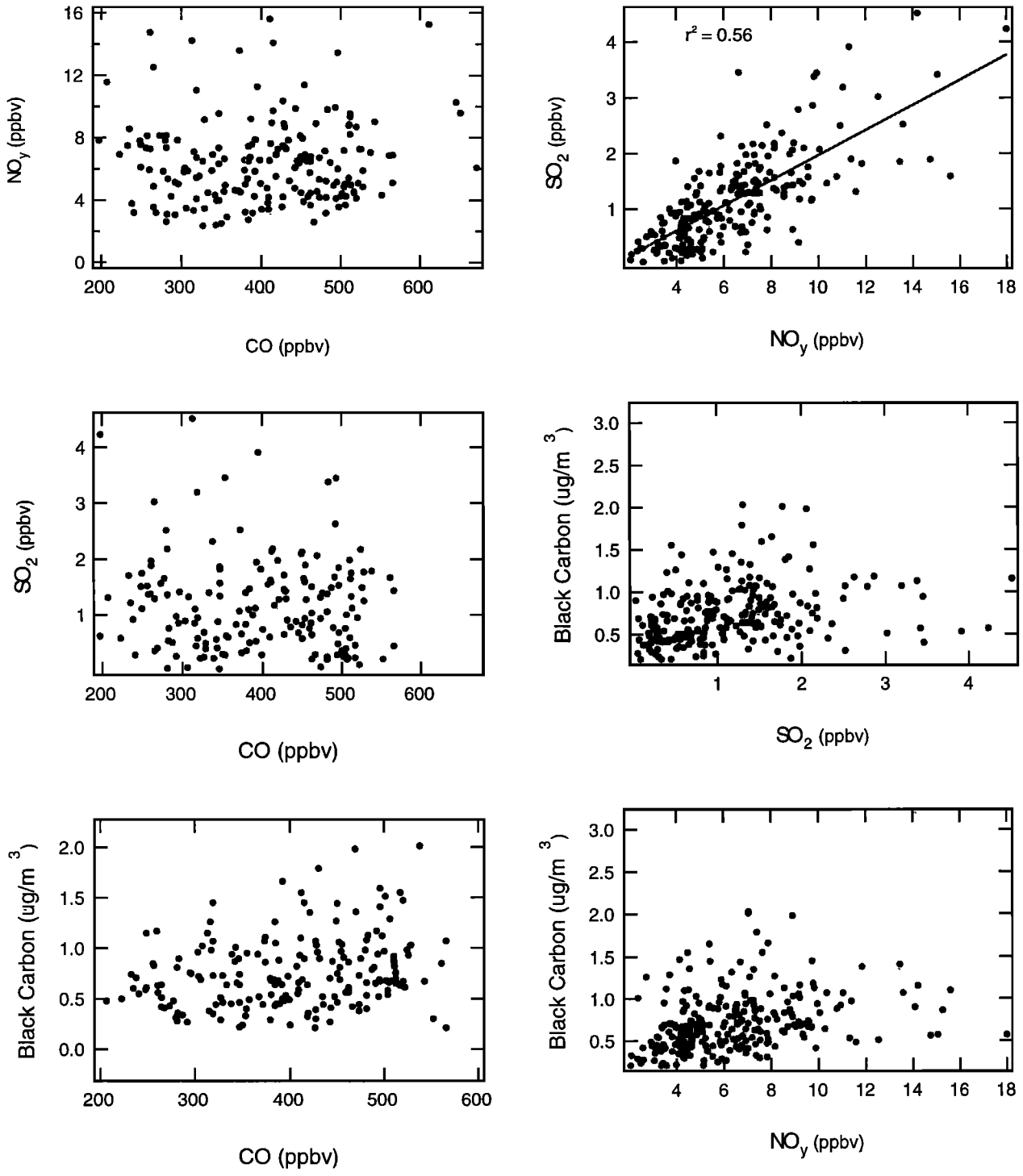

Figure 9. Correlation after applying the wind filter (wind direction >40°, wind speed >5 m/s): (a) relationships of CO with NO_y, SO_2, and black carbon and (b) Correlation of NO_y, SO_2, and black carbon.

during the period from February 17 to March 13, 1994. Periodic surges of continental air had significant impacts on the observed trace gas levels, and cold fronts or troughs brought in high levels of pollutants to the site. Averaged concentrations determined in this study were 34 ± 14 ppbv for O_3, 458 ± 130 ppbv for CO, 9.33 ± 7.84 ppbv for NO_y, and 1.31 ± 1.46 ppbv for SO_2. Their levels (except for O_3) in Hong Kong were higher than those observed at Oki Island and on board a DC-8 plane, indicating that the Hong Kong site was often under the impact of fresh continental emissions, including those of urban Hong Kong, during the winter outflow season. The wintertime concentrations of CO and O_3 were significantly higher than

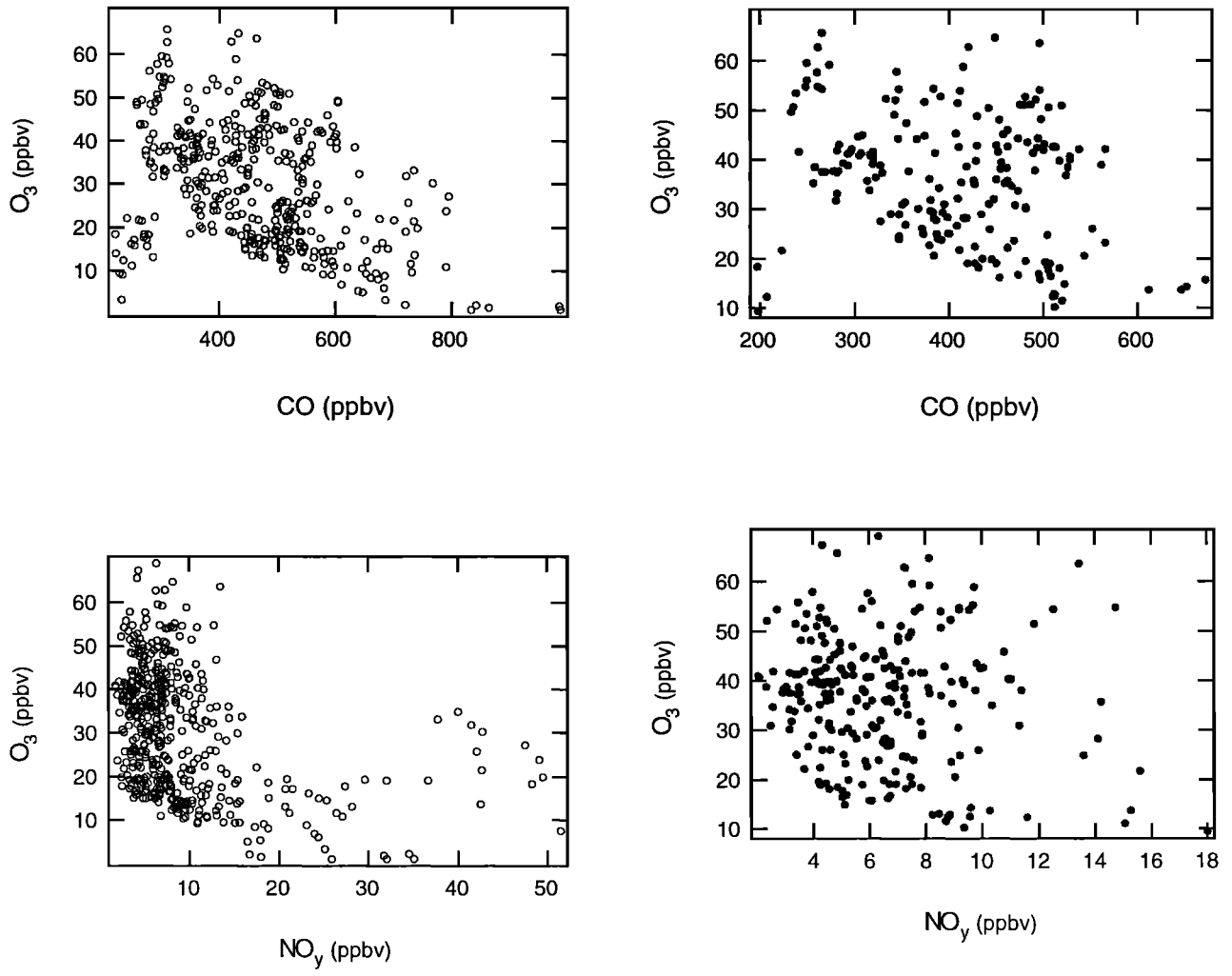

Figure 10. Correlation of ozone with CO and NO_y: (a) all data and (b) wind filter applied (wind direction >40°, wind speed >5 m/s).

the summer (June 1994) values, resulting from dramatic changes in large-scale flow patterns in East Asia from summer to winter seasons.

The variability of CO and, to a lesser extent, O_3 may have been due to both short-range transport of urban plumes and to the long-range transport of pollutants from the continent, whereas the variability in SO_2 and NO_y appeared to be dominated by local sources. CO appeared to be the best chemical indicator, among the gaseous species measured, of the relative intensity of the outflow from the continent.

The correlation of O_3 with CO and NO_y was poor and sometimes showed a negative correlation. This suggests that the air masses sampled were inhomogeneous in terms of the chemical signatures and that O_3 was chemically titrated by anthropogenic pollutants during the early stages of the continental outflow. Overall, SO_2 and NO_y correlated reasonably well and their correlation with CO was not as good. This indicates that elevated SO_2 and NO_y may have been due to sources of common origin.

Isentropic trajectories captured large-scale changes of air masses, indicated also by surface meteorological and chemical data. However, trajectory models offering a finer spatial resolution are needed to study the histories of smaller-scale air masses and to further distinguish between, for example, northerly and northeasterly flows. Furthermore, the reason for the disagreement between the trajectory results and surface winds (sometimes chemical data as well) requires further investigation.

Table 3. Comparison of Winter Mixing Ratios With Summer (June 1994) Values

	Winter		Summer	
	Mean (s.d)	Median	Mean (s.d.)	Median
CO	458 ± 130	455	110 ± 55	87
O_3	34 ± 14	32	22 ± 11	19

Acknowledgments. The team wishes to thank M. Anson, the coordinator of the Polytechnic University Air Monitoring Project. We thank Director of the Hong Kong Observatory for making available the meteorological data, J. Prospero for providing the aerosol data, and J. Merrill for providing the backward air trajectories. T. Wang would like to

express his gratitude to N. D. Sze for coordinating the collaboration between the University of Michigan and the Polytechnic University, and to S C. Liu for his help in the project. We are grateful to W. L. Chang for his help in obtaining the meteorological data. Z. L. Cheng assisted in station operation Technical support from the Department of Civil and Structural Engineering of HKPU was essential to the success of the project. Special thanks go to W. F. Tam and M. C. Ng for their help in setting up and maintaining the station. The friendly cooperation of Hong Kong Telecom in the establishment of the station and in facilitating staff transport is also acknowledged. This research was sponsored by the Hong Kong Polytechnic University and the NASA (through the University of Michigan).

References

Akimoto, H., and H. Narita, Distribution of SO_2, NO_x, and CO_2 emissions from fuel combustion and industrial activities in Asia with 1°x1° resolution, *Atmos. Environ., 28*(2), 213-225, 1994

Akimoto, H., et al., Long-range transport of ozone in the East Asian Pacific Rim region, *J. Geophys. Res., 101*, 1999-2010, 1996.

Arimoto, R , R A. Duce, J. M. Prospero, D L. Savoie, R.W. Talbot, J. E. Dibb, B. G. Heikes, B J Ray, N. F. Lewis, and U. Tomza, Comparisons of trace constituents from ground stations and the DC-8 aircraft during PEM-West B, *J. Geophys. Res.*, this issue.

Galloway, J. N , Atmospheric acidification. Projections for the future. *Ambio, 18*, 161-166, 1989.

Hatakeyama, S., et al., The 1991 PEACAMPOT aircraft observation of ozone, NO_x, and SO_2 over the East China Sea, the Yellow Sea, and the sea of Japan, *J. Geophys. Res., 100* , 23,143-23,151, 1995.

Hoell, J M , D. D. Davis, S. C. Liu, R Newell, M. Shipham, H. Akimoto, R. J McNeal, R. J. Bendura, and J. W. Drewry, The Pacific Exploratory Mission-West A (PEM-West A). September-October 1991, *J. Geophys. Res., 101*, 1641-1654, 1996.

Kajii, Y., and H. Akimoto, Long-range transport of ozone, carbon monoxide, and acidic trace gases at Oki Island, Japan during PEM-West B campaign, *J. Geophys Res.*, this issue

Kondo, Y , M Koike, S. Kawakami, H. B. Singh, H. Nakajima, G. Gregory, D. B Blake, G. Sachse, J. Merrill, and R. Newell, Profiles and partitioning of reactive nitrogen over the Pacific Ocean in winter and early spring, *J. Geophys. Res.*, this issue.

Lam, K. S., T Wang, L. Y. Chan, H. Y. Liu, and M. Anson, Observation of surface ozone and carbon monoxide at a coastal site in Hong Kong, *Proc. Quadrennial Ozone Symposium*, in press, 1996.

Merrill, J. T., E. Arnold, M. Leinen, and C. Weaver, Mineralogy of aeolian dust reaching the North Pacific Ocean, 2, Relationship of mineral assemblages to atmospheric transport patterns, *J. Geophys. Res., 99*, 21,025-21,032, 1994.

Merrill, J. T., Trajectory results and interpretation for PEM-West A, *J. Geophys. Res., 101*, 1679-1690, 1996.

Merrill, J. T., R. E. Newell, and A. S. Bachmeier, A meteorological overview for the Pacific Exploratory Mission-West, Phase B, *J. Geophys. Res.*, this issue

Parrish, D. D., M. Trainer, M. P. Buhr, B A. Watkins, and F. C. Fehsenfeld, Carbon monoxide concentrations and their relation to concentrations of total reactive oxidized nitrogen at two rural sites, *J. Geophys. Res., 96*, 9309-9320, 1991.

Parrish, D. D., J. S. Holloway and F. C. Fehsenfeld, Routine, continuous measurements of carbon monoxide with parts per billion precision, *Environ. Sci. Technol., 28*, 1615-1618, 1994.

Prospero, J. M., and D. L. Savoie, Effect of continental sources on nitrate concentrations over the Pacific Ocean, *Nature, 339*, 687-689, 1989.

Savoie, D. L. and J. M. Prospero, Comparison of oceanic and continental sources of non-sea-salt sulfate over the Pacific Ocean, *Nature, 339*, 685-687, 1989.

Talbot, R. W., et al., Chemical characteristics of continental outflow from Asia to the troposphere over the western Pacific Ocean during February-March 1994: Results from PEM-West B, *J. Geophys. Res.*, this issue.

Warneck, P., *Chemistry of the Natural Atmosphere*, Academic, San Diego, Calif., 1988.

M A. Carroll, Department of Atmospheric, Oceanic, and Space Sciences, University of Michigan, Ann Arbor, MI 48109-2143 (email: mcarroll@umich.edu)

L. Y. Chan, K. S Lam, A. S Y. Lee, and T Wang, Environmental Engineering Unit, Department of Civil and Structural Engineering, The Hong Kong Polytechnic University, Hung Hom, Kowloon, Hong Kong. (email: cetwang@polyu.edu.hk)

(Received August 29, 1996; revised November 17, 1996;
accepted November 17, 1996.)